

Influence of the Membrane Potential on the Free Energy of an Intrinsic Protein

Benoît Roux

Groupe de Recherche en Transport Membranaire, Départements de physique et de chimie, Université de Montréal, Montréal, Québec H3C 3J7, Canada

ABSTRACT A modified Poisson-Boltzmann equation is developed from statistical mechanical considerations to describe the influence of the transmembrane potential on macromolecular systems. Using a Green's function formalism, the electrostatic free energy of a protein associated with the membrane is expressed as the sum of three terms: a contribution from the energy required to charge the system's capacitance, a contribution corresponding to the interaction of the protein charges with the membrane potential, and a contribution corresponding to a voltage-independent reaction field free energy. The membrane potential, which is due to the polarization interface, is calculated in the absence of the protein charges, whereas the reaction field is calculated in the absence of transmembrane potential. Variations in the capacitive energy associated with typical molecular processes are negligible under physiological conditions. The formulation of the theory is closely related to standard algorithms used to solve the Poisson-Boltzmann equation and only small modifications to current source codes are required for its implementation. The theory is illustrated by examining the voltage-dependent membrane insertion of a simple polyaniline α -helix and by computing the electrostatic potential across a 60-Å-diameter sphere meant to represent a large intrinsic protein.

INTRODUCTION

An electrostatic potential difference exists between the cytoplasm of living cells and the extracellular medium because of the unequal distribution of ions on both sides of the cellular membrane. This "membrane potential" underlies numerous important physiological processes, ranging from propagation of the nerve impulse, cell excitability, volume regulation, excitation-secretion coupling, cellular motility, transduction by sensory receptors, and the development of the embryo (Gennis, 1989; Stryer, 1988). By virtue of the long-range nature of the Coulombic interactions, variations in the electrostatic potential generated by the movements of small metal ions across the cell membrane ensure the synchronization of various molecular processes taking place at distances far larger than typical short-range intermolecular forces. For this reason, the membrane potential constitutes a unified communication system for physiological information throughout the cell.

At the microscopic level, the configurational equilibrium and the orientation of membrane-bound proteins is affected by the membrane potential (Blumenthal et al., 1983); e.g., an analysis of sequence of a large series of human type I α -helical membrane proteins showed that residues with positively charged side chains are primarily located on the cytoplasmic side of the cell membrane, whereas residues with negatively charged side chains have a higher propen-

sity to be found on the extracellular side (Landolt-Marti-corena et al., 1993). Furthermore, variations in the membrane potential can induce significant configurational transitions in macromolecular structures. Complex movements of protein segments have been implicated in the transition of colicin 1a from a soluble state to a transmembrane voltage-gated ion channel state (Ghosh et al., 1994; Qiu et al., 1996) and in the open-close kinetics of the *shaker* B potassium channel (Sigworth, 1993; Mannuzzu et al., 1996). In much smaller peptide systems, it is observed that the membrane insertion of melittin (Kempf et al., 1982; Dempsey, 1990; Dempsey et al., 1991) and alamethicin (Cafiso, 1994) is voltage dependent.

In the simplest case of a perfectly planar membrane, the atomic charges associated with the backbone and side chains of an intrinsic protein are expected to interact directly with the (constant) transmembrane electric field. The situation is more complicated when the surface of the membrane, with its associated intrinsic protein, is irregular. To make progress it is necessary to consider the transmembrane potential at a microscopic level. As first discussed by Nernst (1889), a membrane potential appears spontaneously between two ionic solutions separated by a semipermeable membrane as the result of a balance between the entropic tendency to homogenize the system and the necessity to maintain local charge neutrality as much as possible. The struggle between these two opposing forces takes place in the region of the semipermeable membrane, and the potential difference is the result of this interfacial phenomena. Alternatively, it is possible to impose externally a potential difference across an impermeable membrane in the laboratory, using an electromotive force and ion-exchanging electrodes. Both situations correspond to molecular systems in thermodynamic equilibrium.

Received for publication 27 June 1997 and in final form 26 August 1997.

Address reprint requests to Dr. Benoît Roux, Chemistry Department, Université de Montréal, C.P. 6128, Succursale Centre-Ville, Montréal, Québec H3C 3J7, Canada. Tel.: 514-343-7105; Fax: 514-343-7586; E-mail: rouxb@plgcn.umontreal.ca.

© 1997 by the Biophysical Society

0006-3495/97/12/2980/10 \$2.00

In principle, computer simulations of detailed atomic models can provide a powerful approach to study biological macromolecular membrane systems at the microscopic level (Merz and Roux, 1996). However, simple considerations based on classical electrostatics show that, in practice, the membrane potential cannot easily be treated with such an approach. The capacitance of a typical lipid membrane is on the order of $1 \mu\text{F}/\text{cm}^2$, which corresponds to a thickness of $\sim 25 \text{ \AA}$ and a dielectric constant of 2 for the hydrophobic core of a bilayer. In the presence of a membrane potential, the bulk solution remains electrically neutral, and a small charge imbalance is distributed in the neighborhood of the interfaces. For a potential of 100 mV, the net charge per area is $CV = 10^{-7} \text{ Coul}/\text{cm}^2$, which corresponds to only one atomic unit charge per surface of $(130 \text{ \AA})^2$. Because a physiological salt concentration of 150 mM corresponds to approximately one cation-anion pair per volume of $(22 \text{ \AA})^3$, the membrane potential arises from a strikingly small accumulation of net charge relative to the bulk ion density. For molecular dynamics simulations at such a concentration, a minimum membrane system of cross-sectional area of $(130 \text{ \AA})^2$ containing ~ 100 ion pairs would require nearly 40,000 water molecules and more than 500 phospholipids, for a total of more than 180,000 atoms. Despite such a huge atomic system, the membrane potential would be nearly impossible to estimate accurately. The statistical fluctuations would be very large because of the small number of ions giving rise to the interfacial charge imbalance. For a meaningful quantitative description of the membrane potential and its influence on biological macromolecular systems, it is necessary to use a different approach. It is the goal of this paper to develop an effective theoretical formulation of the membrane potential and its influence on the configurational free energy of an intrinsic protein of arbitrary shape, using macroscopic continuum electrostatics.

Macroscopic continuum electrostatics represents a computationally attractive approach to incorporating the dominant effects of solvent (for a recent review, see Honig et al., 1993). The origin of the approximation, in which the environment is represented as a structureless continuum, can be found in the classic work of Gouy (1910), Chapman (1913), Born (1920), and Debye and Hückel (1923). The treatment of macromolecular structures of arbitrary shape is currently made possible by solving the Poisson-Boltzmann (PB) equation numerically with finite-difference algorithms on a discretized grid, using powerful computers (Honig et al., 1993; Klapper et al., 1986; Warwicker and Watson, 1982). In particular, the PB equation was recently used to examine the factors playing a role in the association of proteins with membranes (Ben-Tal et al., 1996). In the present paper, a modified PB equation is developed to describe the environment of a protein embedded in a membrane in the presence of a potential difference. The modified PB equation represents an extension of previous treatment of planar membranes (Lauger et al., 1967; Everitt and Haydon, 1968; Walz et al., 1969). The theory is formulated in the next section, and is illustrated by examining the membrane potential

across a spherical protein embedded in a membrane and the voltage-dependent factors in the process of insertion of a simple polyaniline α -helix.

THEORETICAL FORMULATION

We consider a system in thermodynamic equilibrium consisting of a protein in a fixed configuration \mathbf{R} embedded in an impermeable membrane surrounded by salt solutions ($\mathbf{R} \equiv \{\mathbf{r}_1, \mathbf{r}_2, \dots\}$ represents the coordinates of all of the atoms of the protein). The system is illustrated schematically in Fig. 1. The bulk density of ion of type α is, respectively, $\bar{\rho}_\alpha^{(I)}$ and $\bar{\rho}_\alpha^{(II)}$ on sides I and II of the membrane. An electromotive force V (EMF) is connected to side I and side II by two electrodes. For the sake of simplicity, it is assumed that the EMF and the electrodes are ideal and that one ionic species can be transported directly from one side to the other by going through the circuit. Of course, in a realistic system, the ionic species is not transported per se by the EMF; e.g., with AgCl electrodes, the chloride anion is chemiabsorbed at the surface of the electrode on one side, releasing one electron, which is transported by the EMF to the other side, to yield a chloride anion on the other side (Bockris and Reddy, 1970). However, the exact details of the chemiabsorption process are unimportant in the present treatment and will be ignored.

In thermodynamic equilibrium (McQuarrie, 1976), the probability of any configuration is given according to the Boltzmann factor, $\exp[-\beta U_{\text{tot}}]$, where $U_{\text{tot}} = U - Q_{\text{net}}V$ is the total potential energy of the system, and $\beta = 1/k_B T$ is the reciprocal thermal energy. U is the molecular energy of the system (protein, membrane, and bulk solutions), and $-Q_{\text{net}}V$ is the energy of the total net charge that has transited through the EMF from side I to side II (there is a minus sign because the potential energy of a positive charge is decreasing as it travels from side I to side II through the EMF). Because any macroscopic charge imbalance in the bulk region would yield a prohibitively large energy, the net

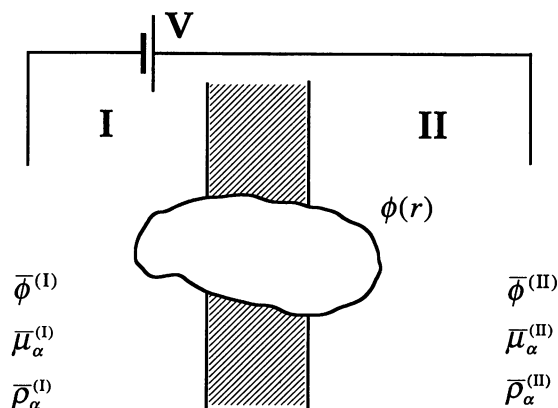


FIGURE 1 Schematic representation of the impermeable membrane system with the intrinsic protein. An electromotive force imposes a potential difference V between side I and side II of the membrane.

charge Q_{net} is very small and the salt solutions remain globally neutral. The equilibrium condition for the ionic species transported by the EMF is

$$\frac{\bar{\rho}_\alpha^{(I)}}{\bar{\rho}_\alpha^{(II)}} = \frac{\exp[-\beta\bar{\mu}_\alpha^{(I)}]}{\exp[-\beta(\bar{\mu}_\alpha^{(II)} - q_\alpha V)]} \quad (1)$$

where $\bar{\mu}_\alpha^{(S)}$ is the excess chemical potential on side S .

The excess chemical potential $\bar{\mu}_\alpha^{(S)}$ represents the reversible work needed to insert one particle on side S in the system. It is composed of two contributions, the intrinsic excess chemical potential, $\Delta\bar{\mu}_\alpha^{(S)}$, arising from local interactions of the ion with the surrounding particles in the bulk, and the interaction with the overall electrostatic potential in the bulk solution (far away from the membrane), $\bar{\phi}^{(S)}$,

$$\bar{\mu}_\alpha^{(S)} = \Delta\bar{\mu}_\alpha^{(S)} + q_\alpha \bar{\phi}^{(S)} \quad (2)$$

The electrostatic potential $\bar{\phi}^{(S)}$ results from the very small net charge imbalance carried by the EMF. The net charge in an electrolyte solution is distributed at the system boundaries. The intrinsic excess chemical potential $\Delta\bar{\mu}_\alpha^{(S)}$ depends on the local composition of the solution and may be expressed formally as a thermodynamic integration with a coupling parameter (Kirkwood, 1935; Yu and Karplus, 1988). As an illustration, a simple description of the intrinsic chemical potential of ions is a combination of the Born model of solvation (Born, 1920) with the theory of Debye and Hückel (1923) for dilute electrolyte solutions (see also McQuarrie, 1976):

$$\Delta\bar{\mu}_\alpha^{(S)} = \frac{q_\alpha^2}{2R_\alpha} \left(\frac{1}{\epsilon_w} - 1 \right) - \frac{q_\alpha^2 \kappa}{2\epsilon_w(1 + \kappa R_\alpha)} \quad (3)$$

where ϵ_w is the dielectric constant of water and $\kappa^2 = 4\pi\beta\sum_\alpha q_\alpha^2 \bar{\rho}_\alpha^{(S)}/\epsilon_w$ is the Debye screening factor on side S . Equations 1 and 2 imply that the difference in the average electrostatic potential between sides I and II is

$$\bar{\phi}^{(II)} - \bar{\phi}^{(I)} = V + \frac{k_B T}{q_\alpha} \ln \left[\frac{\bar{\rho}_\alpha^{(I)}}{\bar{\rho}_\alpha^{(II)}} \right] + \frac{1}{q_\alpha} [\Delta\bar{\mu}_\alpha^{(I)} - \Delta\bar{\mu}_\alpha^{(II)}] \quad (4)$$

The equilibrium properties of the system depend only on the relative chemical potential difference between side I and side II. Experimentally, one tries to control the composition of the solutions so that $\bar{\phi}^{(II)} - \bar{\phi}^{(I)} \approx V$. In the following, we will assume that those conditions are fulfilled and that the difference in electrostatic potential simply corresponds to the EMF.

The free energy of a protein in configuration \mathbf{R} relative to a system without mobile ions and a transmembrane potential may be expressed rigorously as the reversible thermodynamic work needed to construct the system in a step-by-step process. In particular, one can envision the free energy as the reversible work first required to construct the neutral cavity, then impose the membrane potential V , and switch on the electrostatic interactions between the protein and the rest of the system. The total free energy of a protein in a

fixed configuration \mathbf{R} is

$$\mathcal{F}_{\text{tot}}(\mathbf{R}) = \mathcal{F}_{\text{cavity}}(\mathbf{R}) + \mathcal{F}_{\text{elec}}(\mathbf{R}) \quad (5)$$

This free energy decomposition is similar to equation 2 of Ben-Tal et al., (1996). Although such a free energy decomposition is path-dependent (Boresch et al., 1994), it provides a useful and rigorous framework for understanding the different contributions to the solvation free energy and for constructing suitable approximations. The first step, which consists of creating the van der Waals cavity of the protein in the membrane, is very complex. In pure solvent, the cavity contribution is often described in terms of the total solvent-exposed surface of the solute (Ben-Tal et al., 1996). However, it is beyond the purpose of the present analysis to propose a generalization of this contribution in the case of a protein in a membrane. In the simplest approximation, we ignore the influence of the packing of the lipid hydrocarbon chains around the protein, and assume that the cavity contribution is proportional to the protein solvent-exposed area. The second step consists of switching on the electrostatic interactions. It may be expressed as

$$\mathcal{F}_{\text{elec}}(\mathbf{R}) = \int_0^V dV \left\langle \frac{\partial U_{\text{tot}}}{\partial V} \right\rangle_{(V, \lambda=0)} + \int_0^1 d\lambda \left\langle \frac{\partial U_{\text{tot}}}{\partial \lambda} \right\rangle_{(V, \lambda)} \quad (6)$$

$$= - \int_0^V dV \langle Q_{\text{net}} \rangle_{(V, \lambda=0)} + \int_0^1 d\lambda \sum_p q_p \phi(\mathbf{r}_p; V, \lambda)$$

where p indicates the protein charges, and $\phi(\mathbf{r}; V, \lambda)$ is the total average electrostatic potential at point \mathbf{r} with protein charges scaled by the coupling parameter λ .

The total average electrostatic potential results from a superposition of various contributions from the solvent molecules, the lipid headgroups, the mobile counterions, and the protein. In seeking a simple description of the electrostatic potential required for the solvation free energy, we describe the solvent and the membrane in terms of structureless dielectric media. For the present time, we neglect the influence of the net electric field arising from the lipid polar headgroups. The dielectric polarization density at point \mathbf{r} obeys the linear constitutive relation of macroscopic electrostatics:

$$\mathbf{P}(\mathbf{r}) = - \left(\frac{\epsilon(\mathbf{r}) - 1}{4\pi} \right) \nabla \phi \quad (7)$$

where $\epsilon(\mathbf{r})$ is a position-dependent dielectric constant equal to ϵ_w , ϵ_m , and ϵ_p in the bulk water, membrane, and protein regions, respectively. The dielectric boundary of the protein corresponds to the molecular surface, which may be determined by using effective atomic radii (Nina et al., 1997). The Poisson equation for macroscopic media is (Jackson, 1962)

$$\nabla \cdot [\epsilon(\mathbf{r}) \nabla \phi(\mathbf{r})] = -4\pi\lambda \rho^{\text{prot}}(\mathbf{r}) - 4\pi\langle \rho^{\text{ions}}(\mathbf{r}) \rangle_{(V, \lambda)} \quad (8)$$

where $\lambda\rho^{\text{prot}}(\mathbf{r})$ and $\langle\rho^{\text{ions}}(\mathbf{r})\rangle_{(\text{V},\lambda)}$ are the charge density of the protein and mobile counterions, respectively. As indicated by the subscript (V, λ) , the density of the mobile ions changes in the salt solution on both sides of the membrane as a function of the membrane potential V and the coupling parameter λ (in the following, the subscript on the density of mobile ions will be omitted to simplify the notation). To make further progress, it is necessary to have a microscopic description of the ion charge densities in the bulk solutions. The number density of ion of type α at \mathbf{r} on side S is

$$\langle\rho_{\alpha}(\mathbf{r})\rangle = \bar{\rho}_{\alpha}^{(S)} \exp[-\beta(\mu_{\alpha}(\mathbf{r}) - \bar{\mu}_{\alpha}^{(S)})] \quad (9)$$

where $\mu_{\alpha}(\mathbf{r})$ is the excess chemical potential of ion of type α at point \mathbf{r} (i.e., this is equivalent to the reversible work needed to insert the particle at point \mathbf{r}). Neglecting short-range ion-ion interactions (Hansen and McDonald, 1976), the chemical potential of an ion of type α at the point \mathbf{r} is

$$\mu_{\alpha}^{(S)}(\mathbf{r}) = -k_{\text{B}}T \ln[f(\mathbf{r})] + \Delta\bar{\mu}_{\alpha}^{(S)} + q_{\alpha}\phi(\mathbf{r}) \quad (10)$$

where $\phi(\mathbf{r})$ is the total average electrostatic potential at point \mathbf{r} and $f(\mathbf{r})$ is a volume exclusion overlap function equal to zero inside the protein or the membrane, and equal to 1 otherwise.

The total charge density of the mobile ions at any point \mathbf{r} is

$$\langle\rho^{\text{ions}}(\mathbf{r})\rangle = \begin{cases} f(\mathbf{r}) \sum_{\alpha} q_{\alpha} \bar{\rho}_{\alpha}^{(\text{I})} \exp[-\beta q_{\alpha}(\phi(\mathbf{r}) - \bar{\phi}^{(\text{I})})] & \text{if } \mathbf{r} \text{ is on side I} \\ f(\mathbf{r}) \sum_{\alpha} q_{\alpha} \bar{\rho}_{\alpha}^{(\text{II})} \exp[-\beta q_{\alpha}(\phi(\mathbf{r}) - \bar{\phi}^{(\text{II})})] & \text{if } \mathbf{r} \text{ is on side II} \end{cases} \quad (11)$$

For physiological systems (i.e., a membrane potential on the order of 100 mV and a salt concentration of 150 mM), the argument of the exponentials in Eq. 11 is expected to be small and the exponential functions may be linearized. The equilibrium properties of the system depend only on the relative chemical potential difference between side I and side II (see above). Because adding a global offset constant to the electrostatic potential does not influence the ion distribution, we can choose $\bar{\phi}^{(\text{I})} = 0$ and $\bar{\phi}^{(\text{II})} = V$. One has, after linearization,

$$\langle\rho^{\text{ions}}(\mathbf{r})\rangle = \left(\frac{-\bar{\kappa}^2(\mathbf{r})}{4\pi} \right) [\phi(\mathbf{r}) - V\Theta(\mathbf{r})] \quad (12)$$

where $\Theta(\mathbf{r})$ is a Heaviside step function equal to 0 on side I and equal to 1 on side II, and

$$\bar{\kappa}^2(\mathbf{r}) = \begin{cases} 4\pi\beta f(\mathbf{r}) \sum_{\alpha} q_{\alpha}^2 \bar{\rho}_{\alpha}^{(\text{I})} & \text{if } \mathbf{r} \text{ is on side I} \\ 4\pi\beta f(\mathbf{r}) \sum_{\alpha} q_{\alpha}^2 \bar{\rho}_{\alpha}^{(\text{II})} & \text{if } \mathbf{r} \text{ is on side II} \end{cases} \quad (13)$$

which yields the modified Poisson-Boltzmann equation for macroscopic media for the total average electrostatic poten-

tial in the presence of a membrane potential V ,

$$\nabla \cdot [\epsilon(\mathbf{r}) \nabla \phi(\mathbf{r})] - \bar{\kappa}^2(\mathbf{r}) [\phi(\mathbf{r}) - V\Theta(\mathbf{r})] = -4\pi\lambda\rho^{\text{prot}}(\mathbf{r}) \quad (14)$$

Closely related PB equations may be found in previous treatments of planar membranes (Langer et al., 1967; Everitt and Haydon, 1968; Walz et al., 1969).

The solution of the linearized Poisson-Boltzmann equation may be expressed formally as the sum of two separate terms:

$$\phi(\mathbf{r}; V, \lambda) = V\phi_{\text{mp}}(\mathbf{r}) + \lambda\phi_{\text{rf}}(\mathbf{r}) \quad (15)$$

with

$$\phi_{\text{mp}}(\mathbf{r}) = - \int d\mathbf{r}' G(\mathbf{r}, \mathbf{r}') \bar{\kappa}^2(\mathbf{r}') \Theta(\mathbf{r}') \quad (16)$$

and

$$\phi_{\text{rf}}(\mathbf{r}) = - \int d\mathbf{r}' G(\mathbf{r}, \mathbf{r}') 4\pi\rho^{\text{prot}}(\mathbf{r}') \quad (17)$$

where $G(\mathbf{r}, \mathbf{r}')$ is the Green's function, defined by

$$\nabla \cdot [\epsilon(\mathbf{r}) \nabla G(\mathbf{r}, \mathbf{r}')] - \bar{\kappa}^2(\mathbf{r}) G(\mathbf{r}, \mathbf{r}') = \delta(\mathbf{r} - \mathbf{r}') \quad (18)$$

The function $V\phi_{\text{mp}}(\mathbf{r})$ is the solution of Eq. 14, with $\lambda = 0$, corresponding to the electrostatic potential due to the transmembrane voltage V in the absence of the protein charges (ϕ_{mp} is dimensionless). It should be noted that $\phi_{\text{mp}}(\mathbf{r})$ is independent of V and the protein charges (it does depend on $\epsilon(\mathbf{r})$ and $\bar{\kappa}^2(\mathbf{r})$, however). The function $\phi_{\text{rf}}(\mathbf{r})$ is the solution of Eq. 14, with $V = 0$, corresponding to the electrostatic potential due to the protein charges in the absence of any transmembrane voltage. It may be noted that the function $0 \leq \phi_{\text{mp}}(\mathbf{r}) \leq 1$, because of the properties of the differential Eq. 14.

The electrostatic free energy is obtained as two successive thermodynamic integrations, first over V , and then over λ . It is

$$\begin{aligned} \mathcal{F}_{\text{elec}} = & \int_0^V dV \int d\mathbf{r} \Theta(\mathbf{r}) \langle\rho^{\text{ions}}(\mathbf{r})\rangle_{(\text{V},\lambda=0)} \\ & + \int_0^1 d\lambda \sum_{\text{p}} q_{\text{p}} [V\phi_{\text{mp}}(\mathbf{r}_{\text{p}}) + \lambda\phi_{\text{rf}}(\mathbf{r}_{\text{p}})] \end{aligned} \quad (19)$$

where q_{p} and \mathbf{r}_{p} are the protein charges and their position, respectively. The result may be written in the form

$$\mathcal{F}_{\text{elec}} = \frac{1}{2} CV^2 + \left[\sum_{\text{p}} q_{\text{p}} \phi_{\text{mp}}(\mathbf{r}_{\text{p}}) \right] V + \frac{1}{2} \sum_{\text{p}} q_{\text{p}} \phi_{\text{rf}}(\mathbf{r}_{\text{p}}) \quad (20)$$

where C is the capacitance of the system (calculated with $\lambda = 0$, in the absence of protein charges),

$$C = \int d\mathbf{r} \Theta(\mathbf{r}) \left(\frac{-\kappa^2(\mathbf{r})}{4\pi} \right) [\phi_{\text{mp}}(\mathbf{r}) - 1] \quad (21)$$

The capacitance of the system depends on the configuration of the protein, because the local dielectric constant $\epsilon(\mathbf{r})$ and the overlap function $f(\mathbf{r})$ are affected if the protein is not entirely embedded in the membrane region. The second term in Eq. 20 represents the interaction of the protein charges with the membrane potential. It may be expressed as $\mathcal{Q}V$, where \mathcal{Q} corresponds to an effective charge

$$\mathcal{Q} = \sum_p q_p \phi_{\text{mp}}(\mathbf{r}_p) \quad (22)$$

The quantity $\phi_{\text{mp}}(\mathbf{r}_p)$ represents the fraction of the membrane potential seen by the charge q_p . In the case of a perfectly planar system, the electric field across the membrane is constant and $\phi_{\text{mp}}(\mathbf{r}_p)$ is simply the fraction of the membrane thickness (for this reason, it is often referred to as the “electric distance”; Sigworth, 1993; Hille, 1992). More generally, the interaction of the protein charges with the membrane potential may be more complicated than the simple linear field if the shape of the protein-solution interface is irregular. The last term in Eq. 20 is independent of V and corresponds to the self energy plus the reaction field contribution due to the solvent polarization and electrolyte shielding (sometimes called the image interactions and electroosmotic effect; Jordan et al., 1989).

The configurational probability distribution of the subsystem is given by

$$\mathcal{P}(\mathbf{R}) = \frac{\exp[-\beta \mathcal{F}_{\text{tot}}(\mathbf{R})]}{\int d\mathbf{R}' \exp[-\beta \mathcal{F}_{\text{tot}}(\mathbf{R}')] } \quad (23)$$

For simplicity, the configurational space of an intrinsic protein is often described in terms of a number of discrete states s with probabilities (Sigworth, 1993)

$$\mathcal{P}_s = \frac{\exp[-\beta \mathcal{F}_{\text{tot}}(s)]}{\sum_{s'} \exp[-\beta \mathcal{F}_{\text{tot}}(s')]} \quad (24)$$

Last, it can be shown that the charge induced by the protein

on side II of the salt solution in the absence of any membrane potential is related to the electrical distance function:

$$\begin{aligned} \mathcal{Q}^{\text{ext}} &= \int d\mathbf{r} \Theta(\mathbf{r}) \langle \rho^{\text{ions}}(\mathbf{r}) \rangle_{V=0, \lambda=1} \\ &= \int d\mathbf{r} \Theta(\mathbf{r}) \left(\frac{-\bar{\kappa}^2(\mathbf{r})}{4\pi} \right) \phi_{\text{eff}}(\mathbf{r}) \\ &= \int d\mathbf{r} \Theta(\mathbf{r}) \left(\frac{-\bar{\phi}^2(\mathbf{r})}{4\pi} \right) \int d\mathbf{r}' G(\mathbf{r}, \mathbf{r}') (-4\pi) \rho^{\text{prot}}(\mathbf{r}') \\ &= - \int d\mathbf{r}' \phi_{\text{mp}}(\mathbf{r}') \rho^{\text{prot}}(\mathbf{r}') \\ &= - \sum_p q_p \phi_{\text{mp}}(\mathbf{r}_p) \\ &= -\mathcal{Q} \end{aligned} \quad (25)$$

where the property $G(\mathbf{r}, \mathbf{r}') = G(\mathbf{r}', \mathbf{r})$ has been exploited. More generally, it can easily be shown, using similar arguments, that the total charge induced in the solution is

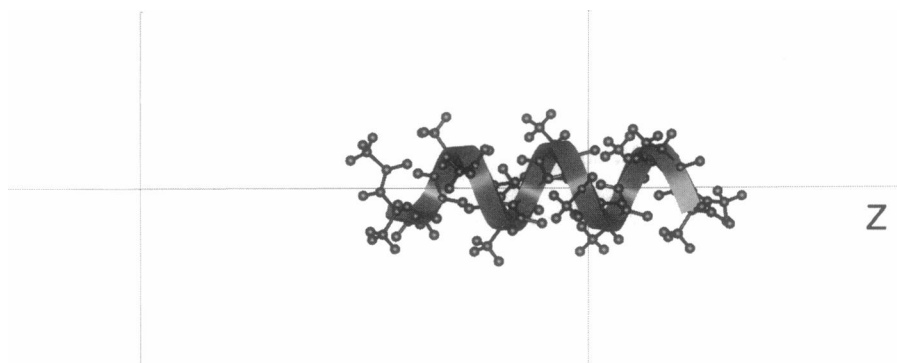
$$\mathcal{Q}^{\text{ext}} = -(\mathcal{Q} + CV) \quad (26)$$

This implies that any charge movements in the interior of the protein will correspond to a current going through the EMF. Such an expression, relating the charge movements in the membrane with the electrical current flowing through the EMF, is used to interpret open-channel ion fluxes as well as gating current in voltage-sensitive ion channel recordings (Sigworth, 1993).

COMPUTATIONAL APPLICATION

To illustrate the present formulation, we consider the free energy of a polyaniline α -helix of 12 residues perpendicular to a membrane surface. The helix-membrane system is illustrated in Fig. 2. To avoid the large desolvation energy associated with charged C- and N-termini, neutral blocking groups were used. The length of the helix is ~ 20 Å. The

FIGURE 2 Membrane insertion of an α -helix of 12 alanine residues. The z axis is parallel to the membrane normal. The position of the helix center of mass is at $z = +10$ Å, the membrane thickness is 25 Å, and the length of the helix is ~ 20 Å. The dielectric constants are $\epsilon_w = 80$, $\epsilon_m = 2$, and $\epsilon_p = 1$. The salt concentration is 150 mM.



isolated helix with blocked end groups is meant to represent a segment of a larger macromolecular structure. The dielectric constant of the bulk water solution was assigned a value of 80. The membrane was assigned a dielectric constant of 2. The dielectric constant of the interior of the protein was assumed to be 1 because the atomic partial charges are presented explicitly (however, the influence of induced electronic polarization is neglected to have an exact correspondence with current biomolecular force fields). The helix, represented in atomic detail with its associated atomic radii and charges, was mapped onto a three-dimensional cubic grid. The dielectric boundary between the solute and the solvent was constructed based on a set of atomic Born radii derived from the average solvent radial charge distribution functions around the 20 amino acids (Nina et al., 1997). The charges were taken from the all-hydrogen PARM22 potential function of CHARMM (Mackerell et al., 1992). The thickness of the membrane is 25 Å. A salt concentration of 150 mM was assumed in the bulk solution, corresponding to a Debye-Hückel screening length $1/\kappa$ of 7.95 Å. It is assumed that the membrane acts as an impenetrable hard wall to the mobile ions, i.e., the volume exclusion function $f(\mathbf{r})$ is zero in the hydrocarbon region (Forsten et al., 1994).

The current model attempts to capture the essential electrostatic feature of the nonpolar, low dielectric, hydrocarbon core of a bilayer and ignores the true complexity of a lipid bilayer (White and Wiener, 1996). For a meaningful description of transmembrane electric fields, it is important to reproduce the magnitude of the membrane capacitance, which is essentially determined by the effective thickness of the low dielectric insulator formed by the membrane. The observed capacitance of membranes is larger than expected, based on the experimental density profile of phospholipid bilayers (White and Wiener, 1996; White, 1978; Waldbillig and Szabo, 1979), suggesting that the insulating region does not correspond to the full thickness of the membrane and that the mobile ions can penetrate extensively into the polar headgroup region.

The nonpolar cavity contribution was calculated using the solvent exposed atomic surface S_p with a smoothed membrane-bulk interface:

$$\mathcal{F}_{\text{cavity}} = - \sum_p \gamma S_p \times \begin{cases} \exp[-(|z_p| - z_m)/\delta z_m] & \text{if } |z_p| > z_m \\ 1 & \text{if } |z_p| < z_m \end{cases} \quad (27)$$

with $\gamma = 0.033 \text{ kcal/mol/Å}^2$, $z_m = 12.5 \text{ Å}$, and $\delta z_m = 2.5 \text{ Å}$. The van der Waals radii from PARM22 (Mackerell et al., 1992) were used to calculate the solvent-exposed surface.

The total electrostatic potential was calculated at each point of the grid by solving the modified PB Eq. 14. The numerical calculations were carried out, using the standard relaxation algorithm (Warwicker and Watson, 1982; Klapper et al., 1986) implemented in the PBEQ facility of

CHARMM (Beglov and Roux, unpublished). Unless specified explicitly, a cubic grid of 150 points of 0.5 Å was used for all of the calculations (the length of the grid is 75 Å). The helix was kept in the center of the box, and the membrane was successively located at different positions along the z axis. Periodic boundary conditions were imposed along in the x and y directions. The analytical solution for a planar membrane was used to set the boundary conditions for the grid in the PB numerical calculations (Lauger et al., 1967; Everitt and Haydon, 1968; Walz et al., 1969). The result for a planar membrane is given in the Appendix.

To compute the capacitance of the system, it was assumed that the induced charge beyond the limits of the system was given by the analytical solution to the case of the planar membrane. The net charges on side I and side II were calculated and agreed almost perfectly, indicating that the size of the grid is sufficient. To compute the reaction field contribution, the standard Poisson-Boltzmann equation was solved with $V = 0$ (zero voltage applied) for the membrane-solution environment and for the vacuum system with a dielectric constant of 1 throughout the box. The (x, y) -periodic boundary of the membrane system was also applied in the vacuum calculations. The solvent reaction field ϕ_{rf} was obtained by subtracting the Coulomb potential computed in vacuum ($\epsilon = 1$) from the total electrostatic potential computed in the membrane system in the absence of a transmembrane potential. To compute the voltage contribution, the modified Poisson-Boltzmann equation was first solved with $\lambda = 0$ (zero charge on the protein). An effective background charge density, corresponding to the offset potential V in Eq. 14, was set in the bulk solution on side II of the membrane to use the same subroutine to solve the Poisson-Boltzmann equation. After the solution was obtained, the charges of the protein were recalled and the interaction energy with the membrane field was calculated as $\sum_p q_p \phi_{\text{mp}}(\mathbf{r}_p)$. The same subroutine was used for computing the free energy contribution from the membrane potential and the reaction field. It should be noted, however, that a factor of $1/2$ must be used in the calculation of the reaction field contribution, in contrast to a factor of 1 used in the calculation of the membrane potential contribution. The different factors arise from the thermodynamic integration in Eq. 20. A few test calculations with different system sizes were performed to examine the convergence of the voltage-induced charge in the double layer and the capacitance. The results with a cubic grid of 150, 160, and 170 points were almost indistinguishable.

RESULTS AND DISCUSSION

The main purpose of the present calculations is to illustrate the magnitude of the various free energy contributions in the presence of a membrane potential. We chose the case of a simple structural element of membrane proteins, an α -helix. The helix axis is parallel to the z axis, with the vector going from the N-terminus to the C-terminus pointing in the $+z$

direction (see Fig. 2). A series of positions along the z axis were examined, as the helix was moved from side I to side II. In Fig. 3 (*top*), the cavity and reaction field contribution to the solvation free energy of the helix is shown. The free energy contributions are given relative to vacuum. As expected, the cavity contribution drives the helix inside the membrane, whereas the electrostatic reaction field contribution is pulling the helix in the bulk solvent region. The electrostatic reaction field contribution to the free energy varies from -44.5 kcal/mol in the bulk to -21.5 kcal/mol in the membrane. The cavity contribution to the free energy varies from 37 kcal/mol in the bulk to 0 kcal/mol in the membrane. The resulting free energy of stabilization of the helix in the membrane relative to the bulk solution is on the order of 13.6 kcal/mol relative to the bulk solution. The electrostatic reaction field contribution to the free energy is not symmetrical with respect to the helix vector. When the helix is located on the left of the membrane (with $z < 0$ Å), the free energy loss due to the buried segment of the helix

groups in the membrane is larger than the corresponding position with the helix on the right of the membrane (with $z > 0$ Å). The reason is that the oxygens of the carbonyl groups (pointing in the $+z$ direction) make a larger contribution to the solvation free energy than the corresponding hydrogens of the amide group (pointing in the $-z$ direction). The results are qualitatively similar to those of Ben-Tal et al. (1996), who examined the free energy of association of an α -helix of 25 alanine residues with a 30-Å-thick membrane and zero membrane potential. Because the present work is focused on the voltage-dependent contributions, we do not discuss further the voltage-independent contributions.

Transmembrane potentials of $+100$ mV and -100 mV were examined, corresponding to a membrane electric field parallel and antiparallel to the helix dipole, respectively. The results are shown in Fig. 3 (*bottom*). The variations in the membrane potential energy contribution are on the order of 1 kcal/mol. The membrane potential energy contribution is a maximum at $z = 0$. Because the length of the helix is ~ 20 Å, the helix is entirely embedded inside the membrane at this location. It is -0.92 kcal/mol in the case where the field is pointing in the direction of the helix dipole, and $+0.92$ kcal/mol in the opposite orientation. In contrast, the variations in the capacitive energy are only on the order of 0.005 kcal/mol (not shown on the figure) and appear to be negligible (see below). The reason is that the total net charge, on the order of 0.242 unit charge for the current system (the area is 5700 Å²), is almost independent on the helix position. Although the total free energy contribution due to the membrane potential is much smaller than that of the reaction field, it is on the order of $k_B T$. Such an energy is large enough to affect the membrane insertion of a helix or induce structural movement in a large macromolecular structure. For comparison, the free energy contribution calculated from the membrane potential of a perfectly planar system is shown. There is a small difference due to the dielectric constant of the protein ($\epsilon_p = 1$), which differs from that of the membrane ($\epsilon_m = 2$). Nevertheless, it may be expected that the membrane potential of a perfectly planar membrane will not be a good approximation in the case of macromolecular structures much larger than a single α -helix (see below).

The influence of the protein shape for markedly nonplanar systems is illustrated by computing the electrostatic potential across a large sphere of 60-Å diameter, which corresponds roughly to a protein of 350–400 residues. Although such a simplified model lacks in atomic details, the calculation remains informative. For instance, we emphasize that the protein atomic partial charges are not used in the calculation of the membrane potential ϕ_{mp} , and only the gross features associated with the protein shape (i.e., $\epsilon(\mathbf{r})$ and $\bar{\kappa}^2(\mathbf{r})$) are involved. Therefore, the calculated ϕ_{mp} would be essentially the same if the van der Waals molecular surface of a detailed atomic model were to result in a large spherical region. The fraction of the transmembrane potential ϕ_{mp} as a function of transverse position z is shown in Fig. 4 for various values of lateral distance d from the

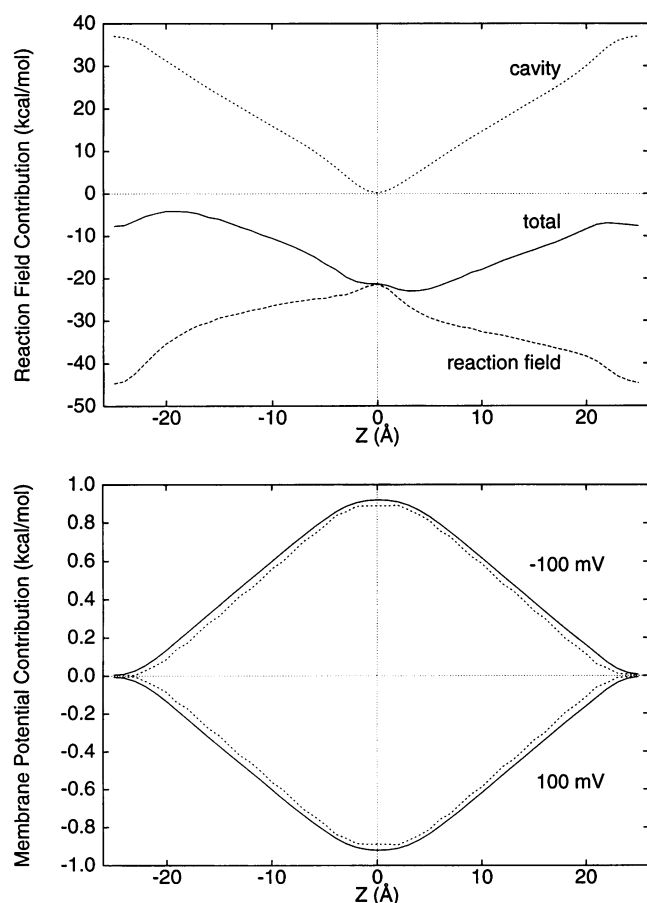


FIGURE 3 Free energy of helix insertion in the membrane. (*Top*) The voltage-independent contributions are shown (cavity and reaction field). (*Bottom*) The voltage-dependent membrane potential contribution for a transmembrane potential of ± 100 mV is shown. The dashed lines represent the interaction energy determined from the analytical solution for a planar membrane. The solid lines correspond to the numerical solution of Eq. 14. The free energy contributions are given relative to vacuum.

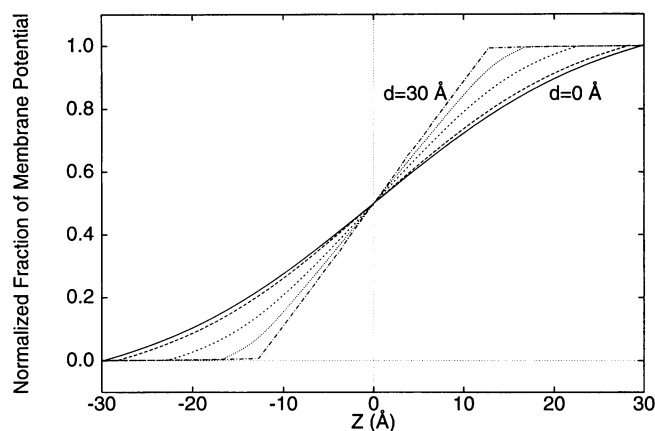


FIGURE 4 Fraction of the transmembrane potential as a function of transverse position z for various values of the lateral distance from the axis intersecting the center of a large spherical protein embedded in an xy -planar membrane. The potential along the z axis for lateral distances $d = 0$, $d = 10$, $d = 20$, $d = 25$, and $d = 30$ Å are shown (only $d = 0$ and $d = 30$ are explicitly indicated; the result for the three intermediate distances are successive from $d = 0$ to $d = 30$). The membrane thickness is 25 Å, and the diameter of the sphere is 60 Å. The dielectric constants $\epsilon_s = 80$, $\epsilon_m = 2$, and $\epsilon_p = 1$. The salt concentration is 150 mM.

axis intersecting the center of the sphere. As expected, the full potential drop takes place over 25 Å at a large distance from the sphere, in the region of the planar membrane. Interestingly, at a distance of 30 Å, which corresponds to the radius of the sphere, the membrane potential profile is already very similar to the analytical solution for a planar membrane. However, variation in the membrane potential across the sphere is very different and happens more slowly. It follows that the energetics of atomic charges located inside the model protein will be affected by both their transverse and lateral positions relative to the center of the sphere. For example, the potential varies by 20% at $z = 12.5$ Å, depending on the lateral position. This result suggests that the energetics of a large macromolecular structure and the population of the conformational states given by Eq. 24 may be affected by internal charge movements both parallel and perpendicular to the membrane normal. This result shows that the observation of voltage-sensitive variations in the conformational states population does not imply that charge movements are taking place solely in the direction of the membrane normal.

For the current system with an area of 5700 Å² and a membrane potential of 100 mV, the capacitive energy for the large 30-Å sphere embedded in the membrane is -0.195 kcal/mol. The corresponding energy for the membrane without the large sphere is -0.275 kcal/mol. Although the absolute magnitude of the energies depends on the area of the membrane, the difference is meaningful. For example, if a protein changed its conformation from a configuration in which it is completely embedded within the membrane to a 30-Å spherical shape, the increase in capacitive energy would be only 0.08 kcal/mol. This calculation dramatically illustrates how the variations in the capacitive energy asso-

ciated with typical molecular processes are completely negligible in such systems under physiological conditions.

SUMMARY

A modified PB equation has been developed to describe the influence of the membrane potential. Using a Green's function formalism, the electrostatic free energy of a membrane protein was expressed as the sum of two terms: a first contribution, which corresponds to the interaction of the protein charges with the membrane potential (calculated in the absence of the protein charges), and a second contribution, which corresponds to a voltage-independent reaction field free energy. The formulation of the theory is closely related to standard algorithms used to solve the PB equation, and only small modifications to current source codes are required for its implementation. The theory was illustrated with the membrane insertion of a simple polyaniline α -helix in the presence of a membrane potential. It was shown that the membrane potential represents a free energy of almost 1 kcal/mol for the insertion of an α -helix. Although the membrane was represented as a planar slab of low dielectric medium in the current application, it would be easy to incorporate an atomic description of the phospholipid bilayer (Peitzsch et al., 1995). This would allow us to take the electric field arising from the interfacial charge due to the lipid polar headgroups into account. However, according to the current analysis, the presence of the membrane interfacial charge would not affect the voltage-dependent contribution to the free energy directly, because the function $\phi_{mp}(\mathbf{r})$ is calculated in the absence of any fixed charges (protein or lipids).

It should be stressed that the current formulation corresponds only to equilibrium situations. In the presence of several permeable ionic species, a membrane potential may also be established, this time as the result of a balance between the relative flux of the various ionic species. This situation, which is traditionally described in terms of the Goldman voltage equation (Goldman, 1943), corresponds to a complex nonequilibrium system. Further work would be required to extend the current equilibrium formulation to nonequilibrium systems.

The current formulation will be particularly useful for examining a variety of molecular processes affected by the membrane potential. Examples are the association of channel-blocking peptides such as charybdotoxin with the potassium channel (Park and Miller, 1992), and the membrane insertion of melittin (Dempsey, 1990) and alamethecin (Cafiso, 1994). Furthermore, it will be interesting to calculate the transmembrane potential acting along the axis of the gramicidin channel by using atomic configurations generated from molecular dynamics simulations (Woelf and Roux, 1996, 1997). Last, the formulation will provide a rigorous basis for assessing the significance of voltage-dependent energetics in models of voltage-gated channels (Sigworth, 1993; Mannuzzu et al., 1996) and membrane

transporters (Panayotova-Heiermann et al., 1994). Work in these various areas is in progress.

APPENDIX: MEMBRANE POTENTIAL FOR PLANAR GEOMETRY

For the sake of completeness, we provide the solution for the planar membrane in detail (Lauger et al., 1967; Everitt and Haydon, 1968; Walz et al., 1969). The system is divided into three regions: region 1 (for $z \leq 0$) and region 3 (for $L \leq z$) are aqueous ionic solutions; region 2 (for $0 \leq z \leq L$) is a hydrocarbon lipid membrane. The dielectric constants of water and the membrane are ϵ_w and ϵ_m , respectively. The screening factor κ is assumed to be the same on the two sides. In each region, the potential obeys

$$\begin{aligned}\phi_1''(z) &= \kappa^2 \phi_1(z) \\ \phi_2''(z) &= 0 \\ \phi_3''(z) &= \kappa^2 (\phi_3(z) - V)\end{aligned}\quad (28)$$

The asymptotic boundary conditions are

$$\begin{aligned}\phi_1(-\infty) &= 0 \\ \phi_3(+\infty) &= V\end{aligned}\quad (29)$$

and the boundary conditions are (Jackson, 1962)

$$\begin{aligned}\phi_1(0) &= \phi_2(0) \\ \epsilon_w \phi_1'(0) &= \epsilon_m \phi_2'(0) \\ \phi_2(L) &= \phi_3(L) \\ \epsilon_m \phi_2'(L) &= \epsilon_w \phi_3'(L)\end{aligned}\quad (30)$$

The solution is

$$\begin{aligned}\phi_1(z) &= Ae^{\kappa z} \\ \phi_2(z) &= A \left[\frac{\epsilon_w}{\epsilon_m} \kappa z + 1 \right] \\ \phi_3(z) &= V - Ae^{-\kappa(z-L)}\end{aligned}\quad (31)$$

where A is a constant equal to

$$A = V \left[2 + \frac{\epsilon_w}{\epsilon_m} \kappa L \right]^{-1} \quad (32)$$

The potential difference at the membrane $\Delta\phi_m = \phi_2(L) - \phi_2(0)$ is

$$\Delta\phi_m = V \left[1 + \frac{2\epsilon_m}{\epsilon_w \kappa L} \right]^{-1} \quad (33)$$

The membrane capacity per unit area is

$$C' = \frac{\epsilon_m}{4\pi L} \left[\frac{2\epsilon_m}{\epsilon_w \kappa L} + 1 \right]^{-1} \quad (34)$$

For very large κ (high screening), the capacity reduces to the well-known result, $\epsilon_m/4\pi L$. The density of ions i on each side of the membrane is given by

$$\langle \rho_\alpha(z) \rangle = \bar{\rho}_\alpha^{(0)} (1 - \beta q_\alpha \phi_1(z)) \quad (35)$$

and

$$\langle \rho_\alpha(z) \rangle = \bar{\rho}_\alpha^{(0)} (1 - \beta q_\alpha (\phi_3(z) - V)) \quad (36)$$

The comments of M. Nina, M. Schumaker, F. J. Sigworth, and O. S. Andersen on the manuscript are gratefully acknowledged. This work was supported by a grant from the MRC of Canada and by the FCAR of Québec. BR is a MRC research fellow.

REFERENCES

- Ben-Tal, N., A. Ben-Shaul, A. Nicholls, and B. H. Honig. 1996. Free energy determinants of alpha-helix insertion into lipid bilayers. *Biophys. J.* 70:1803–1812.
- Blumenthal, R., C. Kempf, J. Van Renswoude, J. N. Weinstein, and R. D. Klausner. 1983. Voltage-dependent orientation of membrane proteins. *J. Cell. Biochem.* 22:55–67.
- Bockris, J. O. M., and A. K. N. Reddy. 1970. *Modern Electrochemistry*. McDonald, London.
- Boresch, S., G. Archontis, and M. Karplus. 1994. Free energy simulations—the meaning of the individual contributions from a component analysis. *Proteins*. 20:25–33.
- Born, M. 1920. Volumen und hydrationswärme der ionen. *Z. Phys.* 1:45–48.
- Cafiso, D. S. 1994. Alamethicin: a peptide model for voltage gating and protein-membrane interactions. *Annu. Rev. Biophys. Biomol. Struct.* 23:141–165.
- Chapman, D. L. 1913. A contribution to the theory of electrocapillarity. *Philos. Mag.* 25:475–481.
- Debye, P., and E. Hückel. 1923. Zur Theorie der Elektrolyte. II. Das Grenzgesetz für die elektrische Leitfähigkeit. *Phys. Z.* 24:305–325.
- Dempsey, C. E. 1990. The actions of melittin on membranes. *Biochim. Biophys. Acta*. 1031:143–161.
- Dempsey, C. E., R. Bazzo, T. S. Harvey, I. Syperek, G. Boheim, and I. D. Campbell. 1991. Contribution of proline-14 to the structure and actions of melittin. *FEBS Lett.* 281:240–244.
- Everitt, C. T., and D. A. Haydon. 1968. Electrical capacitance of a lipid membrane separating two aqueous phases. *J. Theor. Biol.* 18:371–379.
- Forsten, K. E., R. E. Kozack, D. A. Lauffenburger, and S. Subramaniam. 1994. Numerical solution of the nonlinear P-B equation for a membrane-electrolyte system. *J. Phys. Chem.* 98:5580–5586.
- Gennis, R. B. 1989. *Biomembranes: Molecular Structure and Function*. Springer Verlag, New York.
- Ghosh, P., S. F. Mel, and R. M. Stroud. 1994. The domain structure of the ion channel-forming protein colicin Ia. *Nature Struct. Biol.* 1:597–604.
- Goldman, D. E. 1943. Potential, impedance, and rectification in membranes. *J. Gen. Physiol.* 27:37–60.
- Gouy, G. 1910. Sur la constitution de la charge électrique à la surface d'un électrolyte. *J. Phys. (Paris)*. 9:457–468.
- Hansen, J. P., and I. R. McDonald. 1976. *Theory of Simple Liquids*. Academic Press, London.
- Hille, B. 1992. *Ionic Channels of Excitable Membranes*, 2nd Ed. Sinauer Associates, Sunderland, MA.
- Honig, B., K. Sharp, and A.-S. Yang. 1993. Macroscopic models of aqueous solutions: biological and chemical applications. *J. Phys. Chem.* 97:1101–1109.
- Jackson, J. D. 1962. *Classical Electrodynamics*. John Wiley and Sons, New York.
- Jordan, P. C., R. I. Bacquet, J. A. McCammon, and P. Tran. 1989. How electrolyte shielding influences the electrical potential in transmembrane ion channels. *Biophys. J.* 55:1041–1052.
- Kempf, C., R. D. Klausner, J. N. Weinstein, J. Van Renswoude, M. Pincus, and R. Blumenthal. 1982. Voltage-dependent trans-bilayer orientation of melittin. *J. Biol. Chem.* 257:2469–2476.
- Kirkwood, J. G. 1935. Statistical mechanics of fluid mixtures. *J. Chem. Phys.* 3:300–313.

- Klapper, I., R. Hagstrom, R. Fine, K. Sharp, and B. Honig. 1986. Focusing of electric fields in the active site of Cu-Zn superoxide dismutase: effects of ionic strength and amino acid modification. *Proteins*. 1:47–59.
- Landolt-Marticorena, C., K. A. Williams, C. M. Deber, and R. A. F. Reithmeier. 1993. Non-random distribution of amino acids in the trans-membrane segments of human type I single span membrane proteins. *J. Mol. Biol.* 229:602–608.
- Lauger, P., W. Lesslauer, E. Marti, and J. Richter. 1967. Electrical properties of bimolecular phospholipid membranes. *Biochim. Biophys. Acta*. 135:20–32.
- Mackerell, A. D., Jr., D. Bashford, M. Bellot, R. L. Dunbrack, M. J. Field, S. Fischer, J. Gao, H. Guo, D. Joseph, S. Ha, L. Kuchnir, K. Kuczera, F. T. K. Lau, C. Mattos, S. Michnick, D. T. Nguyen, T. Ngo, B. Prodrom, B. Roux, B. Schlenkerich, J. Smith, R. Stote, J. Straub, J. Wior-kiewicz-Kuczera, and M. Karplus. 1992. Self-consistent parametrization of biomolecules for molecular modeling and condensed phase simulations. *Biophys. J.* 61:A143.
- Mannuzzu, L. M., M. M. Moronne, and E. Y. Isacoff. 1996. Direct physical measure of conformational rearrangement underlying potassium channel gating. *Science*. 271:213–216.
- McQuarrie, D. A. 1976. *Statistical Mechanics*. Harper and Row, New York.
- Merz, K. M., and B. Roux, editors. 1996. *Biomolecular Membranes: A Molecular Perspective from Computation and Experiment*. Birkhäuser, Boston.
- Nernst, W. 1889. Die elektromotorische Wirksamkeit der Ionen. *Z. Phys. Chem.* 4:129–181.
- Nina, M., D. Beglov, and B. Roux. 1997. Atomic radii for continuum electrostatics calculations based on molecular dynamics free energy simulations. *J. Phys. Chem.* 101:5239–5248.
- Panayotova-Heiermann, M., D. D. Loo, M. P. Lostao, and E. M. Wright. 1994. Sodium/D-glucose cotransporter charge movements involve polar residues. *J. Biol. Chem.* 269:21016–21020.
- Park, C. S., and C. Miller. 1992. Mapping function to structure in a channel-blocking peptide: electrostatic mutants of charybdotoxin. *Biochemistry*. 31:7749–7755.
- Peitzsch, R. M., M. Eisenberg, K. A. Sharp, and S. McLaughlin. 1995. Calculation of the electrostatic potential adjacent to model phospholipid bilayers. *Biophys. J.* 68:729–738.
- Qiu, X. Q., K. S. Jakes, P. K. Kienker, A. Finkelstein, and S. L. Slatin. 1996. Major transmembrane movement associated with colicin Ia channel gating. *J. Gen. Physiol.* 107:313–328.
- Sigworth, F. J. 1993. Voltage gating of ion channels. *Q. Rev. Biophys.* 27:1–40.
- Stryer, L. 1988. *Biochemistry*, 3rd Ed. W. H. Freeman and Co., New York.
- Waldbillig, H. C., and G. Szabo. 1979. Planar bilayer membranes from pure lipids. *Biochim. Biophys. Acta*. 557:295–305.
- Walz, D., E. Bamberg, and P. Lauger. 1969. Nonlinear electrical effects in lipid bilayer membranes. I. Ion injection. *Biophys. J.* 9:1150–1159.
- Warwicker, J., and H. C. Watson. 1982. Calculation of the electric potential in the active site cleft due to alpha-helix dipoles. *J. Mol. Biol.* 157:671–679.
- White, S. H., and M. C. Wiener. 1996. The liquid crystallographic structure of fluid lipid bilayer membranes. In *Biological Membranes: A Molecular Perspective from Computation and Experiment*. K. M. Merz and B. Roux, editors. Birkhäuser, Boston. 127–144.
- White, W. H. 1978. Formation of solvent free black lipid bilayer from glycerol monooleate dispersed in squalene. *Biophys. J.* 23:337–347.
- Woolf, T. B., and B. Roux. 1996. Structure, energetics and dynamics of lipid-protein interactions: a molecular dynamics study of the gramicidin A channel in a DMPC bilayer. *Protein Struct. Funct. Genet.* 24:92–114.
- Woolf, T. B., and B. Roux. 1997. The binding site of sodium in the gramicidin A channel: comparison of molecular dynamics with solid-state NMR data. *Biophys. J.* 72:1930–1945.
- Yu, H. A., and M. Karplus. 1988. A thermodynamic analysis of solvation. *J. Chem. Phys.* 89:2366–2379.